

Quarkonium production from d+Au to Au+Au collisions

M. Rosati^a on behalf of the PHENIX Collaboration

S.S. Adler⁵, S. Afanasiev²⁰, C. Aidala^{5,10}, N.N. Ajitanand⁴⁶, Y. Akiba^{23,41}, A. Al-Jamel³⁷, J. Alexander⁴⁶, G. Alley³⁸, R. Amirkas¹⁴, K. Aoki²⁷, L. Aphecetche⁴⁸, J.B. Archuleta³⁰, J.R. Archuleta³⁰, R. Armendariz³⁷, V. Armijo³⁰, S.H. Aronson⁵, R. Averbeck⁴⁷, T.C. Awes³⁸, R. Azmoun⁴⁷, V. Babintsev¹⁷, A. Baldissari¹¹, K.N. Barish⁶, P.D. Barnes³⁰, B. Bassalleck³⁶, S. Bathe^{6,33}, S. Batsouli¹⁰, V. Baublis⁴⁰, F. Bauer⁶, A. Bazilevsky^{5,17,42}, S. Belikov^{19,17}, Y. Berdnikov⁴³, S. Bhagavatula¹⁹, M.T. Bjorndal¹⁰, M. Bobrek³⁸, J.G. Boissevain³⁰, S. Boose⁵, H. Borel¹¹, S. Borenstein²⁸, C.L. Britton Jr.³⁸, M.L. Brooks³⁰, D.S. Brown³⁷, N. Brun³¹, N. Bruner³⁶, W.L. Bryan³⁸, D. Bucher³³, H. Buesching^{5,33}, V. Bumazhnov¹⁷, G. Bunce^{5,42}, J.M. Burward-Hoy^{29,30,47}, S. Butsyk⁴⁷, M.M. Cafferty³⁰, X. Camard⁴⁸, J.-S. Chai²¹, P. Chand⁴, W.C. Chang², R.B. Chappell¹⁴, S. Chernichenko¹⁷, A. Chevel⁴⁰, C.Y. Chi¹⁰, J. Chiba²³, M. Chiu¹⁰, I.J. Choi⁵⁵, J. Choi²², S. Chollet²⁸, R.K. Choudhury⁴, T. Chujo⁵, V. Cianciolo³⁸, D. Clark³⁰, Y. Cobigo¹¹, B.A. Cole¹⁰, M.P. Comets³⁹, P. Constantin¹⁹, M. Csanad¹³, T. Csorgo²⁴, H. Cunitz¹⁰, J.P. Cussonneau⁴⁸, D.G. D'Enterria^{10,48}, K. Das¹⁴, G. David⁵, F. Deak¹³, A. Debraine²⁸, H. Delagrange⁴⁸, A. Denisov¹⁷, A. Deshpande⁴², E.J. Desmond⁵, A. Devismes⁴⁷, O. Dietzschi⁴⁴, J.L. Drachenberg¹, O. Drapier²⁸, A. Drees⁴⁷, K.A. Drees⁵, R. du Rietz³², A. Durum¹⁷, D. Dutta⁴, V. Dzhordzhadze⁴⁹, M.A. Echave³⁰, Y.V. Efremenko³⁸, K. El Chenawi⁵², M.S. Emery³⁸, A. Enokizono¹⁶, H. Enyo^{41,42}, M.N. Ericson³⁸, B. Espagnon³⁹, S. Esumi⁵¹, V. Evseev⁴⁰, L. Ewell⁵, D.E. Fields^{36,42}, C. Finck⁴⁸, F. Fleuret²⁸, S.L. Fokin²⁶, B.D. Fox⁴², Z. Fraenkel⁵⁴, S.S. Frank³⁸, J.E. Frantz¹⁰, A. Franz⁵, A.D. Frawley¹⁴, J. Fried⁵, Y. Fukao^{27,41,42}, S.-Y. Fung⁶, S. Gadrat³¹, J. Gannon⁵, S. Garpman^{32,*}, F. Gastaldi²⁸, T.F. Gee³⁸, M. Germain⁴⁸, T.K. Ghosh⁵², P. Giannotti⁵, A. Glenn⁴⁹, G. Gogiberidze⁴⁹, M. Gonin²⁸, J. Gosset¹¹, Y. Goto^{41,42}, R. Granier de Cassagnac²⁸, N. Grau¹⁹, S.V. Greene⁵², M. Grosse Perdekamp^{18,42}, W. Guryn⁵, H.-A. Gustafsson³², T. Hachiya¹⁶, J.S. Haggerty⁵, S.F. Hahn³⁰, H. Hamagaki⁸, A.G. Hansen³⁰, J. Harder⁵, G.W. Hart³⁰, E.P. Hartouni²⁹, M. Harvey⁵, K. Hasuko⁴¹, R. Hayano⁸, N. Hayashi⁴¹, X. He¹⁵, M. Heffner²⁹, N. Heine³³, T.K. Hemmick⁴⁷, J.M. Heuser^{41,47}, M. Hibino⁵³, J.S. Hicks³⁸, P. Hidas²⁴, H. Hiejima¹⁸, J.C. Hill¹⁹, R. Hobbs³⁶, W. Holzmann⁴⁶, K. Homma¹⁶, B. Hong²⁵, A. Hoover³⁷, T. Horaguchi^{41,42,50}, J.R. Hutchins¹⁴, R. Hutter⁴⁷, T. Ichihara^{41,42}, V.V. Ikonnikov²⁶, K. Imai^{27,41}, M. Inaba⁵¹, M. Inuzuka⁸, D. Isenhower¹, L. Isenhower¹, M. Ishihara⁴¹, M. Issah⁴⁶, A. Isupov²⁰, B.V. Jacak⁴⁷, U. Jagadish³⁸, W.Y. Jang²⁵, Y. Jeong²², J. Jia⁴⁷, O. Jinnouchi^{41,42}, B.M. Johnson⁵, S.C. Johnson²⁹, J.P. Jones Jr.³⁸, K.S. Joo³⁴, D. Jouan³⁹, S. Kahn⁵, F. Kajihara⁸, S. Kametani^{8,53}, N. Kamihara^{41,50}, A. Kandasamy⁵, M. Kaneta⁴², J.H. Kang⁵⁵, M. Kann⁴⁰, S.S. Kapoor⁴, K.V. Karadjev²⁶, A. Karar²⁸, S. Kato⁵¹, K. Katou⁵³, T. Kawabata⁸, A. Kazantsev²⁶, M.A. Kelley⁵, S. Kelly^{9,10}, B. Khachaturov⁵⁴, A. Khanzadeev⁴⁰, J. Kikuchi⁵³, D.H. Kim³⁴, D.J. Kim⁵⁵, D.W. Kim²², E. Kim⁴⁵, G.-B. Kim²⁸, H.J. Kim⁵⁵, E. Kinney⁹, A. Kiss¹³, E. Kistenev⁵, A. Kiyomichi^{41,51}, K. Kiyoyama³⁵, C. Klein-Boeing³³, H. Kobayashi^{41,42}, L. Kochenda⁴⁰, V. Kochetkov¹⁷, D. Koehler³⁶, T. Kohama¹⁶, R. Kohara¹⁶, B. Komkov⁴⁰, M. Konno⁵¹, M. Kopytine⁴⁷, D. Kotchetkov⁶, A. Kozlov⁵⁴, V. Kozlov⁴⁰, P. Kravtsov⁴⁰, P.J. Kroon⁵, C.H. Kuberg^{1,30}, G.J. Kunde³⁰, V. Kuriatkov⁴⁰, K. Kurita^{41,42}, Y. Kuroki⁵¹, M.J. Kweon²⁵, Y. Kwon⁵⁵, G.S. Kyle³⁷, R. Lacey⁴⁶, V. Ladygin²⁰, J.G. Lajoie¹⁹, Y. Le Bornec³⁹, A. Lebedev^{19,26}, V.A. Lebedev²⁶, S. Leckey⁴⁷, D.M. Lee³⁰, S. Lee²², M.J. Leitch³⁰, M.A.L. Leite⁴⁴, X.H. Li⁶, H. Lim⁴⁵, A. Litvinenko²⁰, M.X. Liu³⁰, Y. Liu³⁹, J.D. Lopez³⁰, C.F. Maguire⁵², Y.I. Makdisi⁵, A. Malakhov²⁰, V.I. Manko²⁶, Y. Mao^{7,peking,41}, L.J. Marek³⁰, G. Martinez⁴⁸, M.D. Marx⁴⁷, H. Masui⁵¹, F. Matathias⁴⁷, T. Matsumoto^{8,53}, M.C. McCain¹, P.L. McGaughey³⁰, R. McKay¹⁹, E. Melnikov¹⁷, F. Messer⁴⁷, Y. Miake⁵¹, N. Miftakhov⁴⁰, J. Milan⁴⁶, T.E. Miller⁵², A. Milov^{47,54}, S. Mioduszewski⁵, R.E. Mischke³⁰, G.C. Mishra¹⁵, J.T. Mitchell⁵, A.K. Mohanty⁴, B.C. Montoya³⁰, J.A. Moore³⁸, D.P. Morrison⁵, J.M. Moss³⁰, F. Muehlbacher⁴⁷, D. Mukhopadhyay⁵⁴, M. Muniruzzaman⁶, J. Murata^{41,42}, S. Nagamiya²³, J.L. Nagle^{9,10}, T. Nakamura¹⁶, B.K. Nandi⁶, M. Nara⁵¹, J. Newby⁴⁹, S.A. Nikolaev²⁶, P. Nilsson³², A.S. Nyanin²⁶, J. Nystrand³², E. O'Brien⁵, C.A. Ogilvie¹⁹, H. Ohnishi^{5,41}, I.D. Ojha^{3,52}, H. Okada^{27,41}, K. Okada^{41,42}, M. Ono⁵¹, V. Onuchin¹⁷, A. Oskarsson³², I. Ottelund³², K. Oyama⁸, K. Ozawa⁸, D. Pal⁵⁴, A.P.T. Palounek³⁰, C. Pancake⁴⁷, V.S. Pantuev⁴⁷, V. Papavassiliou³⁷, J. Park⁴⁵, W.J. Park²⁵, A. Parmar³⁶, S.F. Pate³⁷, C. Pearson⁵, H. Pei¹⁹, T. Peitzmann³³, V. Penev²⁰, J.-C. Peng^{18,30}, H. Pereira¹¹, V. Peresedov²⁰, A. Pierson³⁶, C. Pinkenburg⁵, R.P. Pisani⁵, F. Plasil³⁸, R. Prigl⁵, G. Puill²⁸, M.L. Purschke⁵, A.K. Purwar⁴⁷, J.M. Qualls¹, J. Rak¹⁹, S. Rankowitz⁵, I. Ravinovich⁵⁴, K.F. Read^{38,49}, M. Reuter⁴⁷, K. Reygers³³, V. Riabov^{40,43}, Y. Riabov⁴⁰, S.H. Robinson³⁰, G. Roche³¹, A. Romana²⁸, M. Rosati¹⁹, E. Roschin⁴⁰, S.S.E. Rosendahl³², P. Rosnet³¹, R. Ruggiero⁵, M. Rumpf²⁸, V.L. Rykov⁴¹, S.S. Ryu⁵⁵, M.E. Sadler¹, N. Saito^{27,41,42}, T. Sakaguchi^{8,53}, M. Sakai³⁵,

^a e-mail: mrosati@iastate.edu

S. Sakai⁵¹, V. Samsonov⁴⁰, L. Sanfratello³⁶, R. Santo³³, H.D. Sato^{27,41}, S. Sato^{5,51}, S. Sawada²³, Y. Schutz⁴⁸, V. Semenov¹⁷, R. Seto⁶, M.R. Shaw^{1,30}, T.K. Shea⁵, I. Shein¹⁷, T.-A. Shibata^{41,50}, K. Shigaki¹⁶, K. Shigaki^{16,23}, T. Shiina³⁰, M. Shimomura⁵¹, A. Sickles⁴⁷, C.L. Silva⁴⁴, D. Silvermyr^{30,32}, K.S. Sim²⁵, C.P. Singh³, V. Singh³, F.W. Sippach¹⁰, M. Sivertz⁵, H.D. Skank¹⁹, G.A. Slegee¹⁹, D.E. Smith³⁸, G. Smith³⁰, M.C. Smith³⁸, A. Soldatov¹⁷, R.A. Soltz²⁹, W.E. Sondheim³⁰, S.P. Sorensen⁴⁹, I.V. Sourikova⁵, F. Staley¹¹, P.W. Stankus³⁸, E. Stenlund³², M. Stepanov³⁷, A. Ster²⁴, S.P. Stoll⁵, T. Sugitate¹⁶, J.P. Sullivan³⁰, S. Takagi⁵¹, E.M. Takagui⁴⁴, A. Taketani^{41,42}, M. Tamai⁵³, K.H. Tanaka²³, Y. Tanaka³⁵, K. Tanida⁴¹, M.J. Tannenbaum⁵, V. Tarakanov⁴⁰, A. Taranenko⁴⁶, P. Tarjan¹², J.D. Tepe^{1,30}, T.L. Thomas³⁶, M. Togawa^{27,41}, J. Tojo^{27,41}, H. Torii^{27,41,42}, R.S. Towell¹, V-N. Tram²⁸, V. Trofimov⁴⁰, I. Tserruya⁵⁴, Y. Tsuchimoto¹⁶, H. Tsuruoka⁵¹, S.K. Tuli³, H. Tydesjo³², N. Tyurin¹⁷, T.J. Uam³⁴, H.W. van Hecke³⁰, A.A. Vasiliev²⁶, M. Vassent³¹, J. Velkovska^{5,47}, M. Velkovsky⁴⁷, W. Verhoeven³³, V. Veszpremi¹², L. Villatte⁴⁹, A.A. Vinogradov²⁶, M.A. Volkov²⁶, E. Vznuzdaev⁴⁰, X.R. Wang¹⁵, Y. Watanabe^{41,42}, S.N. White⁵, B.R. Whitus³⁸, N. Willis³⁹, A.L. Wintenberg³⁸, F.K. Wohn¹⁹, C.L. Woody⁵, W. Xie⁶, Y. Yang⁷, A. Yanovich¹⁷, S. Yokkaichi^{41,42}, G.R. Young³⁸, I.E. Yushmanov²⁶, W.A. Zajc¹⁰, C. Zhang¹⁰, L. Zhang¹⁰, S. Zhou⁷, S.J. Zhou⁵⁴, J. Zimanyi²⁴, L. Zolin²⁰, X. Zong¹⁹

¹ Abilene Christian University, Abilene, TX 79699, USA

² Institute of Physics, Academia Sinica, Taipei 11529, Taiwan

³ Department of Physics, Banaras Hindu University, Varanasi 221005, India

⁴ Bhabha Atomic Research Centre, Bombay 400 085, India

⁵ Brookhaven National Laboratory, Upton, NY 11973-5000, USA

⁶ University of California, Riverside, Riverside, CA 92521, USA

⁷ China Institute of Atomic Energy (CIAE), Beijing, People's Republic of China

⁸ Center for Nuclear Study, Graduate School of Science, University of Tokyo, 7-3-1 Hongo, Bunkyo, Tokyo 113-0033, Japan

⁹ University of Colorado, Boulder, CO 80309, USA

¹⁰ Columbia University, New York, NY 10027 and Nevis Laboratories, Irvington, NY 10533, USA

¹¹ Dapnia, CEA Saclay, 91191 Gif-sur-Yvette, France

¹² Debrecen University, 4010 Debrecen, Egyetem tér 1, Hungary

¹³ ELTE, Eötvös Loránd University, 1117 Budapest, Pázmány P. s. 1/A, Hungary

¹⁴ Florida State University, Tallahassee, FL 32306, USA

¹⁵ Georgia State University, Atlanta, GA 30303, USA

¹⁶ Hiroshima University, Kagamiyama, Higashi-Hiroshima 739-8526, Japan

¹⁷ Institute for High Energy Physics (IHEP), Protvino, Russia

¹⁸ University of Illinois at Urbana-Champaign, Urbana, IL 61801, USA

¹⁹ Iowa State University, Ames, IA 50011, USA

²⁰ Joint Institute for Nuclear Research, 141980 Dubna, Moscow Region, Russia

²¹ KAERI, Cyclotron Application Laboratory, Seoul, South Korea

²² Kangnung National University, Kangnung 210-702, South Korea

²³ KEK, High Energy Accelerator Research Organization, Tsukuba-shi, Ibaraki-ken 305-0801, Japan

²⁴ KFKI Research Institute for Particle and Nuclear Physics (RMKI), 1525 Budapest 114, PO Box 49, Hungary

²⁵ Korea University, Seoul, 136-701, Korea

²⁶ Russian Research Center "Kurchatov Institute", Moscow, Russia

²⁷ Kyoto University, Kyoto 606, Japan

²⁸ Laboratoire Leprince-Ringuet, Ecole Polytechnique, CNRS-IN2P3, Route de Saclay, 91128, Palaiseau, France

²⁹ Lawrence Livermore National Laboratory, Livermore, CA 94550, USA

³⁰ Los Alamos National Laboratory, Los Alamos, NM 87545, USA

³¹ LPC, Université Blaise Pascal, CNRS-IN2P3, Clermont-Fd, 63177 Aubiere Cedex, France

³² Department of Physics, Lund University, Box 118, 221 00 Lund, Sweden

³³ Institut für Kernphysik, University of Muenster, 48149 Muenster, Germany

³⁴ Myongji University, Yongin, Kyonggido 449-728, Korea

³⁵ Nagasaki Institute of Applied Science, Nagasaki-shi, Nagasaki 851-0193, Japan

³⁶ University of New Mexico, Albuquerque, NM 87131, USA

³⁷ New Mexico State University, Las Cruces, NM 88003, USA

³⁸ Oak Ridge National Laboratory, Oak Ridge, TN 37831, USA

³⁹ IPN-Orsay, Universite Paris Sud, CNRS-IN2P3, BP1, 91406 Orsay, France

⁴⁰ PNPI, Petersburg Nuclear Physics Institute, Gatchina, Russia

⁴¹ RIKEN (The Institute of Physical and Chemical Research), Wako, Saitama 351-0198, Japan

⁴² RIKEN BNL Research Center, Brookhaven National Laboratory, Upton, NY 11973-5000, USA

⁴³ St. Petersburg State Technical University, St. Petersburg, Russia

⁴⁴ Universidade de São Paulo, Instituto de Física, Caixa Postal 66318, São Paulo CEP05315-970, Brazil

⁴⁵ System Electronics Laboratory, Seoul National University, Seoul, South Korea

⁴⁶ Chemistry Department, Stony Brook University, Stony Brook, SUNY, NY 11794-3400, USA

⁴⁷ Department of Physics and Astronomy, Stony Brook University, SUNY, Stony Brook, NY 11794, USA

- ⁴⁸ SUBATECH (Ecole des Mines de Nantes, CNRS-IN2P3, Université de Nantes) BP 20722, 44307 Nantes, France
⁴⁹ University of Tennessee, Knoxville, TN 37996, USA
⁵⁰ Department of Physics, Tokyo Institute of Technology, Tokyo, 152-8551, Japan
⁵¹ Institute of Physics, University of Tsukuba, Tsukuba, Ibaraki 305, Japan
⁵² Vanderbilt University, Nashville, TN 37235, USA
⁵³ Waseda University, Advanced Research Institute for Science and Engineering, 17 Kikui-cho, Shinjuku-ku, Tokyo 162-0044, Japan
⁵⁴ Weizmann Institute, Rehovot 76100, Israel
⁵⁵ Yonsei University, IPAP, Seoul 120-749, Korea

Received: 11 April 2005 / Revised version: 26 May 2005 /

Published online: 8 July 2005 – © Springer-Verlag / Società Italiana di Fisica 2005

Abstract. The PHENIX experiment measured J/ψ production in pp, d+Au and Au+Au reactions at $\sqrt{s_{NN}} = 200$ GeV over a wide range of rapidity and transverse momentum. The nuclear modification factor obtained by comparing the d+Au and pp cross sections as a function of rapidity, is consistent with shadowing of the gluon distribution functions. J/ψ production in Au+Au collisions was compared to the production in pp collisions and it was found to be inconsistent with models that predict strong enhancement relative to binary collision scaling.

PACS. 25.75-q, 25.75-Dw,

1 Introduction

Quarkonium production is a probe of the strongly interacting matter created in heavy ion collisions. The behaviour of quarkonium states in a hot and dense medium was proposed as a test of Quark Gluon Plasma formation by Matsui and Satz [1]. Due to their small size, quarkonia can, in principle, survive the deconfinement phase transition. However, the color attraction between the $q\bar{q}$ pair produced in the initial scattering would be screened in the plasma and no bound state can exist at temperatures $T > T_D$ when the screening radius, $1/\mu_D(T)$, becomes smaller than the typical bound-state size [1].

In recent years, a new element has been added to charmonium production in heavy-ion collisions with the realization that $c\bar{c}$ bound states might be recreated in later stages of the reaction. Secondary charmonium production was evaluated in the statistical model for hadron production and it was found to be sizable at RHIC energies [2–8].

The PHENIX experiment at the Relativistic Heavy Ion Collider (RHIC) was specifically designed to make use of high luminosity ion-ion, proton-ion and proton-proton collisions to sample rare physics probes including the J/ψ and other heavy quarkonium states. We review here the first results on J/ψ production in pp, d+Au and Au+Au reactions at $\sqrt{s_{NN}} = 200$ GeV, as reported by PHENIX [9–11].

2 The PHENIX detector

The PHENIX experiment is able to measure J/ψ 's through their dilepton decay in four spectrometers: two central arms covering the mid-rapidity region of $|\eta| < 0.35$ and twice $\pi/2$ in azimuth; and two forward muon arms

covering the full azimuth and $1.2 < |\eta| < 2.4$ in pseudorapidity.

The PHENIX detector is shown schematically in Fig. 1. The central spectrometers are comprised, from the inner radius outward, of a Multiplicity and Vertex Detector (MVD), Drift Chambers (DC), Pixel Pad Chambers (PC), Ring Imaging Cerenkov Counters (RICH), a Time-of-Flight Scintillator Wall (TOF), Time Expansion Chambers (TEC), and two types of Electromagnetic Calorimeters (EMC). This combination of detectors allows for the clean electron identification over a broad range of transverse momentum. Each forward spectrometer consists of a precision muon tracker (MuTr) comprised of three stations of cathode-strip readout chambers followed by a muon identifier (MuID) comprised of multiple layers of steel absorbers instrumented with low resolution planar drift

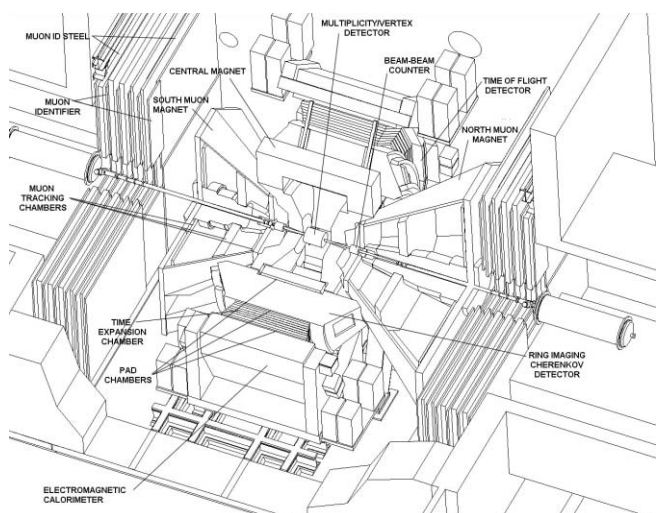


Fig. 1. Detector layout of the PHENIX experiment

* Deceased

† Spokesperson

tubes. Muons at the vertex must have a mean energy of at least 1.9 GeV to reach the MuID system. Further details of the detector design and performance are given in [12].

3 Results

3.1 Proton-proton collisions

The data were recorded during the 2001/2002 (Run2) and 2003 (Run3) runs at $\sqrt{s} = 200$ GeV with 150 nb^{-1} and 350 nb^{-1} pp collisions. Event samples were selected using online triggers and offline reconstruction criteria as described in [9]. Unlike-sign pairs and, for background estimation, like-sign pairs were combined to form invariant mass spectra. In Fig. 2, unlike-sign and like-sign invariant mass spectra from the entire Run2 pp data set are shown together. For electrons, the net yield in the mass region $2.8\text{--}3.4 \text{ GeV}/c^2$ is 46, for muons in the range $2.71\text{--}3.67 \text{ GeV}/c^2$ is 65.

The J/ψ cross sections were determined from the measured yields using

$$B_{ll} \frac{d^2\sigma_{J/\psi}}{dydp_T} = \frac{N_{J/\psi}}{(\int L dt) \Delta y \Delta p_T} \frac{1}{A \epsilon} \quad (1)$$

where $N_{J/\psi}$ is the measured J/ψ yield, $\int L dt$ is the integrated luminosity, B_{ll} is the branching fraction for the J/ψ to either e^+e^- or $\mu^+\mu^-$ pairs (PDG average value 5.9% [13]), $A \epsilon$ is the acceptance times efficiency for detecting a J/ψ . The acceptance times efficiency, $A \epsilon$, shows a dependence on transverse momentum and varies between 0.076 and 0.034 in the muon spectrometers and 0.026 and 0.010 in the electron spectrometers. The J/ψ rapidity distribution obtained by combining the dielectron and dimuon measurements is shown in Fig. 3, with the muon arm data divided into two rapidity bins. A fit to a shape generated with PYTHIA using the GRV94HO parton distribution functions is performed and gives a total cross section, multiplied by the dilepton branching ratio B_{ll} of 5.9%, equal to:

$$B_{ll} \times \sigma_{pp}^{J/\psi} = 159 \text{ nb} \pm 8.5\% \text{ (fit)} \pm 12.3\% \text{ (abs)} \quad (2)$$

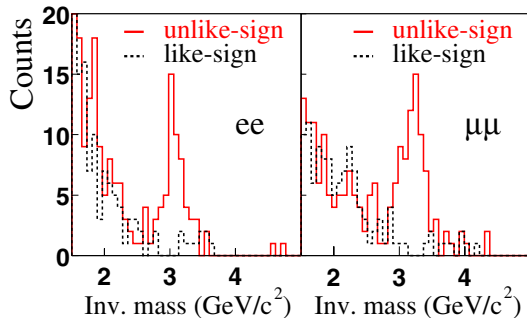


Fig. 2. The invariant mass spectra for dielectron and dimuon pairs in the Run 2 data sample. Unlike-sign pairs are shown as solid lines, like-sign pairs as dashed lines

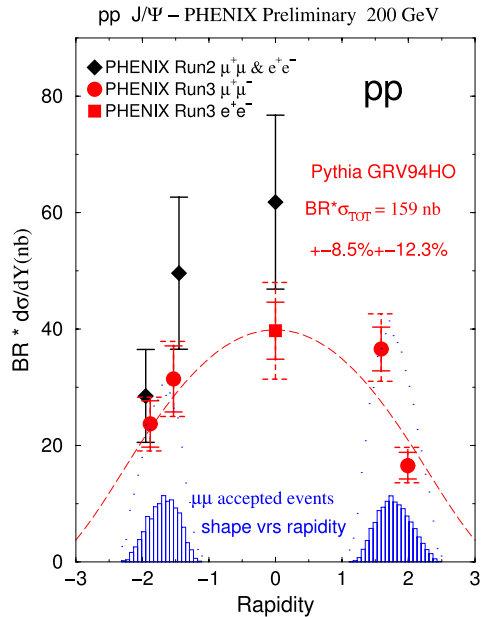


Fig. 3. J/ψ differential cross section, multiplied by the dilepton branching ratio, versus rapidity, as measured by the central and muon spectrometers

where the first uncertainty comes from the fit and thus includes both the statistical and point-to-point systematics. The second uncertainty accounts for absolute systematic errors.

3.2 d+Au collisions

A preliminary analysis of the data recorded during the 2003 run, at $\sqrt{s} = 200$ GeV, with 2.74 nb^{-1} d+Au collisions, is now available. In d+Au collisions, PHENIX is able to measure J/ψ production at forward, backward and central rapidity probing moderate to low x regions of the Au nucleus. The covered rapidity region spans the expected shadowing, anti-shadowing and no shadowing regions. The ratio between the J/ψ yields observed in d+Au and pp collisions divided by 2×197 is shown in Fig. 4. Solid error bars represent statistical and point to point systematic uncertainties. The dashed error bars stand for the systematic uncertainties common to one spectrometer. An additional 13.4% global error bar is not displayed.

While this ratio is close to unity at backward rapidity, it is significantly lower at forward rapidity, where parton distributions are expected to be shadowed in a heavy nucleus. Theoretical predictions [14, 15] are displayed on the figure for comparison. The shape is consistent with shadowing at low x and less suppression at larger x . Unfortunately, the statistical and systematic error bars make it difficult to distinguish among various shadowing models and models with various amounts of nuclear absorption.

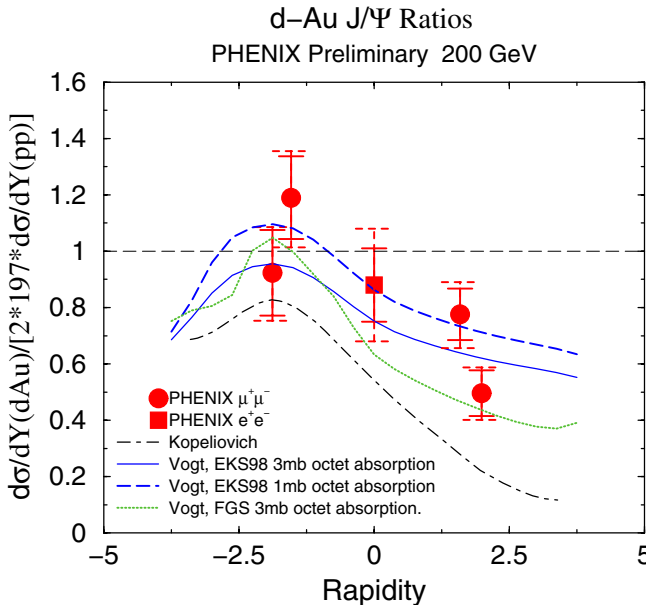


Fig. 4. Ratio between $d\text{-Au}$ and pp J/ψ differential cross sections, divided by 2×197 , versus rapidity

3.3 Au+Au collisions

The Au+Au data at $\sqrt{s_{NN}} = 200$ GeV used in this analysis were recorded during Run 2 at RHIC in the fall of 2001. Using the unlike-sign and like-sign invariant mass spectra from the entire Run 2 data set we measured a J/ψ net yield in the mass region $2.8\text{--}3.4$ GeV/c^2 of 13. For three exclusive centrality bins, 0–20%, 20–40%, and 40–90% of the total Au+Au cross section, we determined the branching fraction of $J/\psi \rightarrow l^+l^-$ ($B_l=5.9\%$ [13]) times the invariant yield at mid-rapidity $dN/dy|_{y=0}$.

In Fig. 5 we show the results from the three Au+Au centrality bins and the proton-proton data normalized per binary nucleon-nucleon collision as a function of the number of participating nucleons. Note that for proton-proton reactions, there are two participating nucleons and one binary collision. Despite the limited statistical significance of these first J/ψ results, we can address some important physics questions raised by the numerous theoretical frameworks in which J/ψ rates are calculated. The binary scaling expectations are shown as a gray band. We also show a calculation of the suppression expected from “normal” nuclear absorption using $\sigma_{\text{abs}} = 4.4$ mb [16] and 7.1 mb [17].

The NA50 suppression pattern relative to binary scaling [18,19], normalized to match our proton-proton data point at 200 GeV, is also included. The data disfavor binary scaling while they are consistent with “normal” nuclear absorption alone and with the NA50 suppression pattern measured at lower energies, within the large statistical errors.

A model calculation [7,8] including just the “normal” nuclear and plasma absorption components at RHIC energies is shown in Fig. 6 (lower solid line). The higher temperature (T) and longer time duration of the system

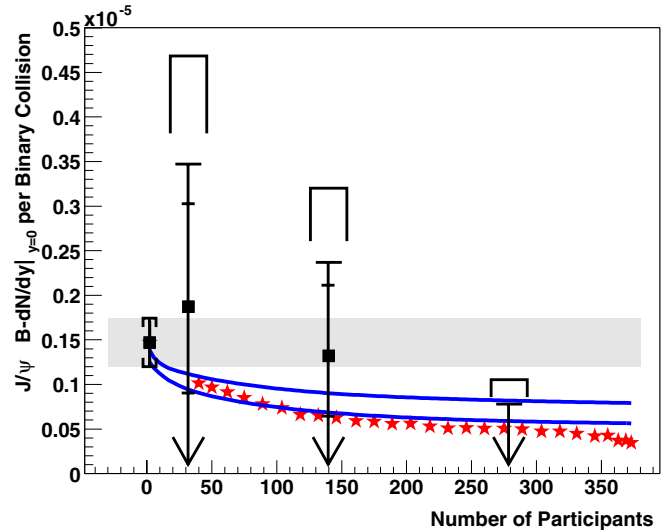


Fig. 5. The J/ψ yield per binary collision is shown for proton-proton reactions and three exclusive centrality ranges of Au+Au reactions, all at $\sqrt{s_{NN}} = 200$ GeV. The solid line is the theoretical expectation from “normal” nuclear absorption with $\sigma_{cc-N} = 4.4$ mb (upper curve) and 7.1 mb (lower curve). The stars are the J/ψ per binary collision measured by the NA50 experiment at lower collision energy. In order to compare the shapes of the distribution, we have normalized the NA50 data to match the central value for our proton-proton results

at RHIC lead to a predicted larger J/ψ suppression with respect to the binary collision scaling.

Many recent theoretical calculations also include the possibility for additional late stage re-creation or coalescence of J/ψ states. In [7,8], both break-up and creation reactions $D + \bar{D} \leftrightarrow J/\psi + X$ are included. At the fixed target CERN energies this represents a very small contribution due to the small charm production cross section. However, at RHIC energies, where around 10 $c\bar{c}$ pairs are produced in central Au+Au collisions, the contribution is significant.

The sum of the initial production, absorption, and re-creation is shown in Fig. 6 (upper solid curve).

A different calculation [6] assumes the formation of a quark-gluon plasma in which the mobility of heavy quarks in the deconfined region leads to increased $c\bar{c}$ coalescence. This leads to a very large enhancement of J/ψ production at RHIC energies for the most central reactions. The model considers the plasma temperature (T) and the rapidity width (Δy) of charm quark production as input parameters. Shown in Fig. 6, as dashed curves, are the calculation results for $T = 400$ MeV and $\Delta y = 1, 2, 3$, and 4. The narrower the rapidity window in which all charm quarks reside, the larger the probability for J/ψ formation. For all these parameters, this model predicts J/ψ enhancement relative to binary collisions scaling, which is disfavored by our data.

Another framework for determining quarkonia yields is to assume a statistical distribution of charm quarks that may then form quarkonia. A calculation assuming ther-

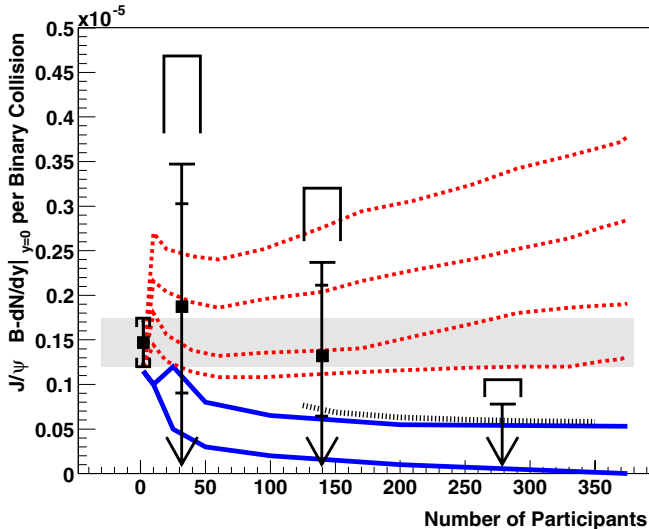


Fig. 6. Same data as previous figure. The lowest curve is a calculation including “normal” nuclear absorption in addition to substantial absorption in a high temperature quark-gluon plasma [7,8]. The curve above this one includes backward reactions that recreate J/ψ mesons. The statistical model [5] result is shown as a dotted curve for mid-central to central collisions. The four dashed curves are from the plasma coalescence model [6] for $T = 400$ MeV and different charm rapidity widths

mal, but not chemical, equilibration [5], is shown in Fig. 6 as a dotted curve.

Significantly larger data sets are required to address the various models that are still consistent with our first measurement. Key tests will be the p_T and x_F dependences of the J/ψ yield, and how these compare with other quarkonium states such as the ψ' .

4 Outlook

PHENIX has unprecedented capabilities for the study of quarkonium production due to the much higher center of mass energy and the wider kinematic coverage with respect to previous experiments. From the Au+Au and Cu+Cu collisions recorded in the years 2004 and 2005, we expect $\approx 10\,000$ and ≈ 1000 J/ψ events in the muon and central arms, respectively. These data sets will allow us to measure J/ψ production at RHIC as a function of rapidity, transverse momentum and explore the suppression pattern relative to binary scaling.

References

1. T. Matsui, H. Satz, Phys. Lett. B **178**, 416 (1986)
2. M. Gazdzicki, M.I. Gorenstein, Phys. Rev. Lett. **83**, 4009 (1999)
3. P. Braun-Munzinger, J. Stachel, Phys. Lett. B **490**, 196 (2000)
4. M.I. Gorenstein, A.P. Kostyuk, H. Stöcker, W. Greiner, Phys. Lett. B **509**, 277 (2001)
5. A. Andronic, P. Braun-Munzinger, K. Redlich, J. Stachel, Phys. Lett. B **571**, 36 (2003)
6. R.L. Thews, M. Schrödter, J. Rafelski, Phys. Rev. C **63**, 054905 (2001)
7. L. Grandchamp, R. Rapp, Phys. Lett. B **523**, 60 (2001)
8. L. Grandchamp, R. Rapp, Nucl. Phys. A **709**, 415 (2002)
9. S.S. Adler et al. (PHENIX Coll.), Phys. Rev. Lett. **92**, 051802 (2004)
10. R.G. de Cassagnac (PHENIX Coll.), J. Phys. G **30**, S1341 (2004)
11. S.S. Adler et al. (PHENIX Coll.), Phys. Rev. C **69**, 014901 (2004)
12. K. Adcox et al. (PHENIX Coll.), Nucl. Instrum. Meth. A **499**, 469 (2003)
13. Particle Data Group, Phys. Rev. D **66**, 010001 (2002)
14. S.R. Klein, R. Vogt, Phys. Rev. Lett. **91**, 142301 (2003)
15. B. Kopeliovich, A. Tarasov, J. Hufner, Nucl. Phys. A **696**, 669 (2001)
16. M.C. Abreu et al. (NA50 Coll.), Phys. Lett. B **553**, 167 (2003)
17. D. Kharzeev, C. Lourenço, M. Nardi, H. Satz, Z. Phys. C **74**, 307 (1997)
18. M.C. Abreu et al. (NA50 Coll.), Phys. Lett. B **477**, 28 (2000)
19. M.C. Abreu et al. (NA50 Coll.), Phys. Lett. B **521**, 195 (2001)
20. M.C. Abreu et al., (NA50 Coll.), Phys. Lett. B **477**, 28 (2000); M.C. Abreu et al., (NA50 Coll.), Phys. Lett. B **521**, 195 (2001)